Published January, 1996

Properties and Variability of Soil and Trench Fill at an Arid Waste-Burial Site

B. J. Andraski *

ABSTRACT

Arid sites commonly are assumed to be ideal for long-term isolation of wastes. Information on properties and variability of desert soils is limited, however, and little is known about how the natural site environment is altered by installation of a waste facility. During fall construction of two test trenches next to the waste facility on the Amargosa Desert near Beatty, NV, samples were collected to: (i) characterize physical and hydraulic properties of native soil (upper 5 m) and trench fill, (ii) determine effects of trench construction on selected properties and vertical variability of these properties, and (iii) develop conceptual models of vertical variation within the soil profile and trench fill. Water retention was measured to air dryness ($\psi = 2 \times 10^6$ cm water suction). The 15 300-cm pressure-plate data were omitted from the analysis because water-activity measurements showed the actual suction values were significantly less than the expected 15 300-cm value (avg. difference = 8550 ± 2460 cm water). Trench construction significantly altered properties and variability of the natural site environment. For example, water content ranged from 0.029 to 0.041 $m^3\ m^{-3}$ for fill vs. 0.030 to 0.095 $m^3\ m^{-3}$ for soil; saturated hydraulic conductivity was $\approx 10^{-4}$ cm s^{-1} for fill vs. 10^{-2} to $\approx 10^{-4}$ cm s^{-1} for soil. Statistical analyses showed that the native soil may be represented by three major horizontal components and the fill by a single component. Under initial conditions, calculated liquid conductivity (K_l) plus isothermal vapor conductivity (K_v) for the upper two soil layers and the trench fill was $\approx 10^{-13}$ cm s^{-1}, and K_l was $\leq K_v$. For the deeper (2–5 m) soil, total conductivity was $\approx 10^{-10}$ cm s^{-1}, and K_l was $> K_v$. This study quantitatively describes hydraulic characteristics of a site using data measured across a water-content range that is representative of arid conditions, but is seldom studied.

INCREASING VOLUMES of radioactive and other hazardous wastes produced each year are of major concern in that new sites will be required for disposal of these wastes. The primary objective for waste-burial facilities is to limit exposure of the public to hazardous wastes for 100 to 10 000 yr.

Sites in arid regions commonly are assumed to be ideal for long-term isolation of wastes (Reith and Thomson, 1992) because the natural environment has features that can reduce the potential for waste migration (e.g., low precipitation, high evapotranspiration, thick unsaturated zone). The complex processes and interacting factors affecting water flow at arid sites, however, are not well understood (Gee and Hillel, 1988; Nativ, 1991; Andraski, 1992). Depending on specific but commonly transient conditions, water movement through either liquid or vapor flow may occur in response to matric suction and temperature gradients. Under dry conditions, movement in the vapor phase is likely to be an important transport mechanism for certain contaminants (e.g., tritium, ^{14}C, radon). Evaluation of flow processes at arid sites requires the use of numerical models (Fayer and Gee, 1992; Scanlon and Milly, 1994) because of these complexities. Adequate and complete data needed for numerical simulation of flow processes generally are lacking, however, because of difficulties in characterizing the physical and hydraulic properties of the commonly dry, stony desert soils (Mehuys et al., 1975; Russo, 1983; Andraski, 1991). Few attempts have been made to measure hydraulic properties across the extreme range of water content observed at arid sites. Although recent work at active or proposed arid waste-burial sites has increased our knowledge of soil properties and flow processes in undisturbed arid settings (Fischer, 1992; Istok et al., 1994; Scanlon and Milly, 1994), little is known about how, or to what degree, the natural site environment is altered by the installation of a waste-burial facility.

This work was prompted by the need to better define and quantify the factors and processes affecting waste isolation at a representative arid waste-burial site. The specific objectives of this study were to: (i) characterize the physical and hydraulic properties of native soil (upper 5 m) and trench fill, (ii) determine the effects of burial-trench construction on selected physical and hydraulic properties and vertical variability of these properties, and (iii) quantitatively develop preliminary conceptual models of vertical variation within the native soil profile and the trench fill for use in numerical simulations of unsaturated flow at the site.

MATERIALS AND METHODS

The study site is adjacent to the commercial waste-burial facility on the Amargosa Desert, about 17 km southeast of Beatty, NV, and 20 km east of Death Valley National Park. On the basis of disposal-facility records (R. Marchand, US Ecology, Inc., 1991, personal communication) and data collected at the study site (Wood and Andraski, 1995), annual precipitation during 1981 to 1992 averaged 108 mm. Depth to the water table ranges from 85 to 115 m below land surface (Fischer, 1992). Sediments in the area are largely alluvial and fluvial deposits (Nichols, 1987). Surface soils are mapped as the Yermo–Arizo association (W.E. Dollarhide, USDA-SCS, 1987, personal communication). The Yermo soils are loamy-skeletal, mixed (calcareous), thermic Typic Torriorthents, and the Arizo soils are sandy-skeletal, mixed, thermic Typic Torriorthents. Vegetation in the area is sparse; creosote bush [*Larrea tridentata* (DC.) Cov.] is the dominant species. The waste facility has been used for the burial of low-level radioactive waste (1962–1992) and hazardous chemical waste (1970–present). The low-level radioactive waste facility was the first such commercially operated site in the USA. Steps used in construction of the low-level radioactive waste burial trenches include excavation and stockpiling of native soil, emplacement of waste, and backfilling with previously stockpiled, uncompacted soil. Dimensions of the trenches have changed since the facility opened in 1962. Until the mid-1970s, trenches were about 1 to 3 m wide, 2 to 6 m deep, and 100 to 200 m long. Trenches constructed later are 30 to 90 m wide, 15 m deep, and 250 m long.

Two test trenches were constructed during September 1987 using methods that simulate those used during active disposal at the low-level radioactive waste-burial facility. The test trenches were excavated by backhoe to about 4 m in all three dimensions

U.S. Geological Survey, 333 W. Nye Lane, Carson City, NV 89706. Received 1 Mar. 1995. *Corresponding author (andraski@usgs.gov).

Published in Soil Sci. Soc. Am. J. 60:54–66 (1996).

and soil-filled drums were used to simulate containers of waste (Fig. 1). Additional details on construction and instrumentation of the test trench site are given by Andraski (1990).

During excavation of the trenches and instrumentation of soil below the 4-m depth, five soil deposits within the upper 5 m were visually identified by texture, cohesiveness, and color. Layers were designated 1 (surface) to 5 (deepest). Soil Layer 1 is about 0.75 to 1 m thick and each of the four underlying layers is ≈ 1 m thick. Five 0.5-m-thick trench-fill layers were defined: 1, cover; 2 and 3, upper and lower half of the upper fill, respectively; 4 and 5, upper and lower half of the lower fill, respectively. The 0.5-m thickness corresponds with the thickness of layers produced during backfilling. For each trench, three to nine volumetric and associated bulk samples were collected from each layer of native soil and trench fill. A total of 92 volumetric samples and 92 associated bulk samples were collected. Volumetric determinations were based on the rubber-balloon method, except that those for the native soil between 4.4 and 5 m deep were based on core data (Andraski, 1991). Although undisturbed core samples are preferred for subsequent laboratory analyses, the rubber-balloon method was chosen because it is more reliable for the extreme ranges of rock-fragment content and soil cohesiveness at the site.

The bulk density of soil plus rock fragments, ρ_T (referred to hereafter as field bulk density), was calculated by dividing oven-dry mass by sample volume. Field volumetric water content (θ_T) was calculated as the product of gravimetric water content and ρ_T. Particle-size distribution was measured by sieve and hydrometer methods (Gee and Bauder, 1986). Rock-fragment bulk density (ρ_r) was determined from rock-fragment particle density and porosity. Rock-fragment particle density was measured by water pycnometry (Blake and Hartge, 1986) and porosity was determined by oven drying the sample for 24 h after vacuum saturation. Rock-fragment particle density and ρ_r averaged (n = 92) 2.50 ± 0.04 and 2.33 ± 0.05 Mg m^{-3}, respectively. Volumetric rock-fragment content (R_v) was calculated by $R_v = \rho_T(R_g/\rho_r)$, where R_g is total gravimetric rock-fragment content. Fine-soil bulk density (ρ_b) was calculated by $\rho_b = \rho_T(1 - R_g)/(1 - R_v)$.

Rock fragments were removed and hydraulic properties were measured on the fine-soil (<2-mm-diam.) fraction. Each sample was packed to its calculated fine-soil bulk density prior to analysis. Saturated hydraulic conductivity of the fine soil (K_s) was measured by the constant-head method (Klute and Dirksen, 1986) using samples (6 cm long, 5.4-cm diam.) that had been slowly wetted from the bottom up. Saturated hydraulic conductivity of soil plus rock fragments, K_{sT} (referred to hereafter as field saturated conductivity), was estimated using an empirical equation proposed by A.J. Peck and J.D. Watson, 1979, unpublished data:

$$K_{sT} = K_s\, 2(1 - R_v)/(2 + R_v) \qquad [1]$$

Equation [1] was derived using a heat-flow analogy for soil with noninteracting spherical inclusions and assumes zero hydraulic conductivity for the inclusions (i.e., rock fragments). Dunn and Mehuys (1984) evaluated the Peck and Watson equation and found good agreement between estimated and measured decreases in K_{sT} with increasing R_v values. Soil-water retention functions were determined using desorption data. Because matric suctions at the field site range from near zero to >80 000 cm of water (Andraski, 1990), water retention was measured using different methods to cover the entire range. Pressure-plate methods (Klute, 1986) on 3-cm-long by 5.4-cm-diam. samples

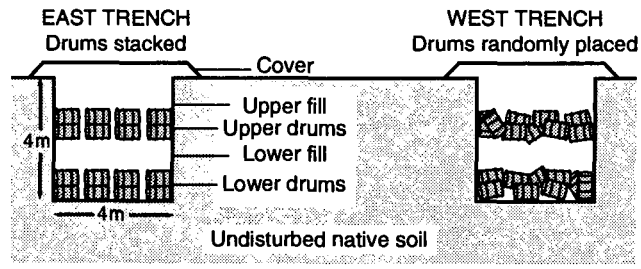

Fig. 1. General design of two test trenches constructed using methods that simulate those used during active disposal at the low-level radioactive waste burial facility on the Amargosa Desert near Beatty, NV.

were used to determine water content at pressures of 20, 41, 82, 336, 1020, 5100, and 15 300 cm of water. Immediately following the 15 300-cm pressure-plate measurement, a water-activity meter (Gee et al., 1992) and a series of air-drying steps (0, 4, 8, and 504 h) were used to extend water-retention measurements to air dryness (2 × 10^6 cm of water). Water-activity measurements made immediately after the 15 300-cm pressure-plate measurements showed that the actual suction values averaged 8550 ± 2460 cm of water less than the expected 15 300-cm value. A paired t-test (Steel and Torrie, 1980) showed that the difference between measurement methods was significant ($P > |t| = 0.001$). This discrepancy is assumed to be due to lack of equilibration for the pressure-plate measurement. Thus, the 15 300-cm pressure-plate data were not used in further analysis.

Water retention was described using the two-parameter junction model of Rossi and Nimmo (1994):

$$\begin{aligned} \theta/\theta_s &= \theta_I = 1 - c(\psi/\psi_o)^2 && 0 \le \psi \le \psi_i \\ \theta/\theta_s &= \theta_{II} = (\psi_o/\psi)^\lambda && \psi_i \le \psi \le \psi_j \\ \theta/\theta_s &= \theta_{III} = \alpha \ln(\psi_d/\psi) && \psi_j \le \psi \le \psi_d \end{aligned} \qquad [2]$$

where θ is volumetric water content and ψ is suction expressed as a pressure head (cm of water). The parameter θ_s was measured and, here, it represents the water content of fine soil obtained at $\psi = 0$ following slow upward wetting. The parameter ψ_d, which represents a finite value of suction where $\theta = 0$, was calculated (9.2 × 10^6 cm of water) by applying the Kelvin equation to the conditions of oven drying (Ross et al., 1991)

$$\psi_d = -(RT/Mg)\ln(h_a p_{sa}/p_{so}) \qquad [3]$$

where R is the ideal gas constant (8.31 × 10^7 ergs mol^{-1} K^{-1}; erg = 10^7 J), T is temperature (K), M is molecular weight of water (18.01 g mol^{-1}), g is gravitational constant (980.6 cm s^{-2}), h_a is humidity of air outside the oven (dimensionless ratio), and p_{sa} and p_{so} are saturated vapor pressures of water at ambient laboratory air and oven temperatures (kPa), respectively. The model was fit to retention data of each sample and ψ_o and λ were optimized using nonlinear least squares analysis (SAS Institute, 1988). The ψ_o parameter may be regarded as a scaling factor related to air-entry suction and λ is a shape factor. The parameters c, ψ_i, ψ_j, and α were determined as analytical functions of ψ_o and λ. Field water content (θ_T) and field-saturated water content (θ_{sT}) then were estimated using

$$\theta_T = \theta\,(1 - R_v)$$

and

$$\theta_{sT} = \theta_s\,(1 - R_v) \qquad [4]$$

where rock fragments are assumed to hold negligible water.

The experiment for determining the effects of burial-trench

construction on selected physical and hydraulic properties and their vertical (layer to layer) variability was a 2 × 5 factorial (two materials: soil and trench fill; five layers) with two replicates (trenches) in a completely random design (Steel and Torrie, 1980). Presence and orientation of waste drums were not considered factors in the experimental design. Analysis of variance (ANOVA) procedures and contrasts (SAS Institute, 1988) were applied to test main-factor and interaction effects on the physical and hydraulic properties by using a split-plot model, with material as the main-plot factor and layer as the split-plot factor (Steel and Torrie, 1980). Analyses were done using subsample averages, with three to nine subsamples for each material and layer combination. In addition to testing the overall interaction effect, orthogonal (linearly independent) contrasts were used to partition the overall interaction effect and test individual interactions between materials and contiguous layers. The $P = 0.05$ significance level was used for testing material, layer, and material × layer interaction effects.

Prior to applying ANOVA procedures, residual analyses were used to test the assumptions of normally distributed and homogeneous error and to determine the need for data transformation. The Shapiro–Wilk W statistic was used to test the assumption of normally distributed experimental errors and residual plots were used to test error homogeneity as described by Fernandez (1992). Within materials, layers were assumed independent (no autocorrelated error) because of the randomness of the processes that formed the native soil profile and the random backfilling process.

Means were compared using Fisher's least significant difference test (LSD) (Steel and Torrie, 1980). The split-plot experimental design generally gives higher precision for split-plot (layer) comparisons, but at the cost of lower precision for main-plot (material) comparisons. For this experiment, however, the increased precision for tests between layers is beneficial for assessing vertical variability, which can greatly affect water movement. If the ANOVA indicates significant interactions, then factors cannot be interpreted independently and paired comparisons are made between the mean values for specific material and layer combinations. Under these conditions, (i) LSD is used to determine significance of the difference between two layer means within a material, (ii) LSD′ is used to determine significance of the difference between two material means within the same layer or different layers, and (iii) the $P = 0.01$ significance level is used to control the error rate of multiple-mean comparisons. For the experimental design used in this study, the calculation of LSD′ is necessary because comparisons across materials involve two error terms, one associated with material and one with layer (Steel and Torrie, 1980). For comparisons within materials, however, LSD is the appropriate test statistic because it accounts only for the error associated with layer.

Results of the statistical analyses were used to quantitatively develop preliminary conceptual models of vertical variation within the native soil profile and trench fill. Hydraulic properties measured in the study then were described for each component of the conceptual models.

RESULTS AND DISCUSSION

Characteristics of Native Soil and Trench Fill Layers

Descriptive statistics for physical properties of the native soil layers are given in Table 1. Fine-soil texture of the five soil layers is: 1, loamy sand; 2, coarse sand; 3, 4, and 5, coarse sandy loam. Layer 4, with a clay content of 18.3%, approached the texture of a sandy clay loam. Compared with Layer 1, R_g and R_v values

Table 1. Descriptive statistics for particle-size distribution, total gravimetric and volumetric rock-fragment contents (R_g and R_v), field (soil plus rock fragments) and fine-soil bulk densities (ρ_T and ρ_b), and field water content (θ_T) during sampling for layers within native soil.

			Sand†						Rock-fragment content							
	Clay	Silt	Total	Very fine	Fine	Medium	Coarse	Very coarse	R_g total	2–4.75 mm	4.75–12.5 mm	>12.5 mm	R_v total	ρ_T	ρ_b	θ_T
	% of <2-mm diam.								% of total					Mg/m³		m³/m³
									Layer 1 (n = 18)							
Mean	6.1	14.1	79.8	16.4	27.2	15.1	11.9	9.2	21.9	8.7	9.9	3.3	14.0	1.46	1.31	0.030
Min.	2.5	10.4	73.5	9.0	14.0	11.1	6.5	3.3	8.7	3.7	3.8	0.0	4.9	1.23	1.08	0.011
Max.	8.0	19.0	85.6	24.4	36.2	23.1	21.7	17.4	42.9	17.1	19.0	8.6	29.6	1.63	1.42	0.060
SD	1.5	2.6	3.4	4.6	7.2	3.1	4.2	4.3	11.4	5.0	5.1	2.6	8.1	0.11	0.09	0.016
									Layer 2 (n = 6)							
Mean	2.8	2.5	94.7	1.5	6.0	23.8	37.4	26.0	58.6	21.2	27.6	9.8	49.1	1.91	1.54	0.043
Min.	1.7	0.0	90.8	1.0	4.2	20.5	32.1	23.5	38.3	18.6	15.3	4.4	27.2	1.70	1.29	0.038
Max.	5.0	7.1	96.7	2.2	7.5	27.9	45.4	27.3	73.6	23.8	39.7	14.7	66.5	2.09	1.78	0.050
SD	1.2	2.6	2.6	0.4	1.4	3.3	5.0	1.4	14.6	2.1	9.4	4.5	15.4	0.14	0.17	0.005
									Layer 3 (n = 6)							
Mean	13.6	5.7	80.7	1.8	9.1	28.2	24.3	17.3	59.9	21.2	28.3	10.4	45.4	1.77	1.30	0.071
Min.	8.2	3.5	73.0	1.0	4.1	19.4	20.5	9.6	49.4	19.0	17.8	6.9	37.9	1.65	1.11	0.058
Max.	18.8	9.0	88.4	3.5	14.7	37.7	26.8	22.3	68.8	24.1	36.7	18.1	51.9	1.93	1.48	0.085
SD	4.6	2.5	5.6	0.9	4.1	7.2	2.6	4.9	7.3	2.3	6.5	4.3	5.7	0.10	0.18	0.009
									Layer 4 (n = 6)							
Mean	18.3	6.0	75.7	1.9	6.8	20.7	27.4	18.9	62.7	20.4	29.7	12.6	51.0	1.86	1.41	0.095
Min.	14.8	4.2	72.8	0.7	2.6	14.2	19.9	14.0	45.1	13.8	21.4	6.0	36.5	1.74	1.10	0.076
Max.	20.3	6.9	79.7	3.4	11.8	27.9	34.0	30.6	74.0	24.1	40.0	21.3	59.7	2.07	1.86	0.137
SD	2.1	1.1	2.4	1.1	3.6	5.2	5.9	6.4	11.0	3.6	6.2	6.2	8.9	0.14	0.29	0.022
									Layer 5 (n = 14)							
Mean	12.9	4.9	82.2	1.7	6.3	14.6	31.4	28.2	54.8	19.2	22.1	13.5	36.7	1.56	1.10	0.078
Min.	8.9	2.3	74.6	0.7	3.3	8.2	21.4	18.5	33.1	14.0	9.9	1.4	22.6	1.33	0.85	0.062
Max.	19.6	8.5	88.2	3.0	9.6	23.8	37.1	38.0	66.0	38.2	31.3	27.3	46.0	1.62	1.41	0.101
SD	3.2	1.9	4.0	0.7	2.1	5.2	4.8	6.1	10.5	6.3	6.6	8.1	7.6	0.09	0.16	0.011

† Particle diameters are clay, <0.002 mm; and silt, 0.002–0.05 mm; sand fractions are very fine, 0.05–0.1 mm; fine, 0.1–0.25 mm; medium, 0.25–0.5 mm; coarse, 0.5–1 mm; and very coarse, 1–2 mm.

were at least 2.5 times greater for the four gravelly subsurface layers. The layer-to-layer differences in particle-size distribution are indicative of the processes active in forming the soil profile. In relation to subsurface layers, the high silt and fine sand contents and low rock-fragment content of Layer 1 reflect eolian deposition and cumulate soil development beneath a desert pavement (McFadden et al., 1987). Textural stratification below Layer 1 reflects alluvial and fluvial processes. Mean ρ_T values ranged from 1.46 to 1.91 Mg m^{-3} and, within layers, values were quite uniform (CVs <10%). Mean θ_T at the time of sampling ranged from 0.030 to 0.095 m^3 m^{-3} and was least for the surface layer. The small θ_T value for soil Layer 1 is related to the time of sampling (September; high antecedent plant water use, low antecedent precipitation) and the small value for Layer 2 reflects the coarse texture. For subsurface layers, θ_T increased with clay content.

Descriptive statistics for physical properties of the trench fill layers are given in Table 2. Textural classification for each of the five fill layers is gravelly loamy coarse sand. Among layers, mean ρ_T values ranged from 1.59 to 1.74 Mg m^{-3} and, within layers, values showed little variation (CVs <10%). Mean θ_T at the time of sampling ranged from 0.029 to 0.041 m^3 m^{-3}.

Descriptive statistics for hydraulic properties of the native soil layers are given in Table 3. Application of Eq. [1] to account for R_v resulted in K_{sT} values that were 21 to 65% less than the associated K_s values. Within layers, K_{sT} was highly variable (CVs ≈70–180%), but the variation was consistent with that reported by Istok et al. (1994) for other alluvial soils in southern Nevada (CVs ≈70–205%). Mean θ_{sT} for Layer 1 was about 25 to 75% greater than θ_{sT} for the subsurface layers. Mean values for the Rossi–Nimmo fitting parameter ψ_o ranged from near zero to about 20 cm of water and λ ranged from 0.13 to 0.27.

Descriptive statistics for hydraulic properties of the trench fill layers are given in Table 4. Within layers, K_{sT} was about 40% less than K_s, and K_{sT} showed less variation (CVs ≈47–69%) than that observed for native soil. For the remaining hydraulic properties, values were relatively uniform among and within layers. Mean ψ_o values were from 12 to 17 cm of water and λ was 0.21 or 0.22.

The retention-curve fitting parameters were positively correlated with silt content of the materials. Correlation coefficients (r) determined using the mean values given in Tables 1 through 4 (n = 10), were r = 0.855 ($P > |r|$ = 0.002) for ψ_o and silt content, and r = 0.881 ($P > |r|$ = 0.0007) for λ and silt content.

Trench Construction Effects on Soil Properties and Vertical Variability

The effects of burial-trench construction on selected physical and hydraulic properties and vertical variability of these properties were tested using ANOVA procedures. Physical properties evaluated were clay, silt, sand, R_v, ρ_T, and θ_T at time of sampling and hydraulic properties were K_{sT}, θ_{sT}, ψ_o, and λ.

Table 2. Descriptive statistics for particle-size distribution, total gravimetric and volumetric rock-fragment contents (R_g and R_v), field (soil plus rock fragments) and fine-soil bulk densities (ρ_T and ρ_b), and field water content (θ_T) during sampling for layers within trench fill.

			Sand†						Rock-fragment content							
	Clay	Silt	Total	Very fine	Fine	Medium	Coarse	Very coarse	R_g total	2–4.75 mm	4.75–12.5 mm	>12.5 mm	R_v total	ρ_T	ρ_b	θ_T
	% of <2-mm diam.								% of total					– Mg/m^3 –		m^3/m^3
								Layer 1 (n = 12)								
Mean	6.4	9.4	84.2	5.5	17.7	21.4	21.5	18.1	36.8	12.6	16.9	7.3	25.5	1.61	1.36	0.029
Min.	4.2	6.3	78.2	2.8	7.4	14.6	17.0	11.0	16.6	4.3	6.7	3.3	11.7	1.29	1.11	0.016
Max.	8.9	15.0	86.8	10.5	24.4	28.0	28.6	26.8	48.2	19.3	22.8	13.0	37.3	1.79	1.56	0.042
SD	1.2	2.4	2.4	1.8	5.4	3.8	3.6	5.0	10.8	4.8	5.1	2.4	8.4	0.14	0.16	0.009
								Layer 2 (n = 12)								
Mean	5.6	8.9	85.5	5.1	17.5	23.1	21.0	18.8	40.9	14.3	18.2	8.4	29.3	1.65	1.38	0.031
Min.	3.4	6.3	81.7	3.0	9.6	18.8	16.8	13.5	24.6	8.1	10.9	3.9	14.5	1.40	1.14	0.021
Max.	8.9	11.6	88.4	7.6	24.6	29.0	28.0	22.6	50.4	18.4	24.1	13.0	38.9	1.79	1.60	0.043
SD	1.6	1.6	2.1	1.6	4.7	3.3	3.2	3.1	7.2	3.0	3.9	3.0	6.0	0.12	0.14	0.008
								Layer 3 (n = 6)								
Mean	6.7	8.6	84.7	5.7	20.9	21.3	19.5	17.3	38.9	13.9	16.6	8.4	28.8	1.74	1.49	0.030
Min.	5.9	6.8	83.3	3.7	15.5	17.8	15.9	13.0	30.0	11.4	13.9	4.7	20.6	1.68	1.46	0.021
Max.	7.7	10.7	86.9	7.9	24.6	24.7	23.1	21.4	44.9	16.7	20.7	11.6	34.7	1.80	1.54	0.047
SD	0.7	1.6	1.6	1.4	3.9	2.6	3.1	3.3	5.3	2.1	2.3	2.8	4.8	0.04	0.03	0.010
								Layer 4 (n = 6)								
Mean	8.3	7.6	84.1	4.5	10.4	26.1	23.6	19.5	49.4	17.3	24.1	8.0	36.0	1.69	1.34	0.038
Min.	5.5	3.4	78.5	3.1	6.9	24.4	20.2	14.2	37.4	15.1	18.8	3.4	28.5	1.57	1.06	0.032
Max.	10.5	12.2	89.9	5.6	14.3	28.5	26.5	26.0	59.6	23.0	29.6	11.0	44.0	1.92	1.61	0.043
SD	2.3	3.2	4.7	1.0	2.4	1.7	2.4	4.5	7.7	3.0	4.2	2.6	6.1	0.12	0.19	0.004
								Layer 5 (n = 6)								
Mean	7.3	6.8	85.9	4.0	11.3	25.6	23.6	21.4	37.3	14.7	17.7	4.9	25.2	1.59	1.34	0.041
Min.	6.0	4.4	83.4	2.6	8.2	17.1	19.4	14.6	32.6	11.3	15.7	2.9	21.4	1.52	1.21	0.037
Max.	8.9	10.6	88.4	5.2	13.9	34.8	26.5	28.9	47.0	18.8	22.6	6.9	31.4	1.68	1.44	0.046
SD	1.3	2.5	1.7	0.9	2.2	6.5	2.8	5.0	5.0	2.9	2.6	1.5	3.5	0.07	0.08	0.004

† Particle diameters are clay, <0.002 mm, and silt, 0.002–0.05 mm; sand fractions are very fine, 0.05–0.1 mm; fine, 0.1–0.25 mm; medium, 0.25–0.5 mm; coarse, 0.5–1 mm; and very coarse, 1–2 mm.

Table 3. Descriptive statistics for fine-soil and field (soil plus rock fragments) saturated hydraulic conductivities (K_s and K_{sT}), fine-soil and field saturated water contents (θ_s and θ_{sT}), and Rossi-Nimmo retention model fitting parameters (ψ_o, λ) for layers within native soil.

	K_s	K_{sT}	θ_s	θ_{sT}	ψ_o	λ
	cm/s		m^3/m^3		cm water	
		Layer 1 (n = 18)				
Mean	1.0×10^{-3}	7.9×10^{-4}	0.339	0.293	20.2	0.27
Min.	3.0×10^{-4}	2.5×10^{-4}	0.259	0.204	15.9	0.22
Max.	8.6×10^{-3}	6.4×10^{-3}	0.391	0.366	27.6	0.35
SD	1.9×10^{-3}	1.4×10^{-3}	0.034	0.049	3.7	0.04
		Layer 2 (n = 6)				
Mean	4.5×10^{-2}	2.3×10^{-2}	0.324	0.165	0.03	0.13
Min.	6.3×10^{-3}	1.6×10^{-3}	0.270	0.106	0.001	0.09
Max.	1.1×10^{-1}	6.2×10^{-2}	0.365	0.240	0.09	0.17
SD	4.0×10^{-2}	2.4×10^{-2}	0.036	0.054	0.04	0.02
		Layer 3 (n = 6)				
Mean	1.0×10^{-2}	4.7×10^{-3}	0.373	0.205	1.1	0.14
Min.	1.8×10^{-3}	7.1×10^{-4}	0.308	0.162	0.01	0.08
Max.	2.5×10^{-2}	1.2×10^{-2}	0.426	0.254	2.5	0.17
SD	8.6×10^{-3}	4.1×10^{-3}	0.044	0.041	1.0	0.03
		Layer 4 (n = 6)				
Mean	1.1×10^{-2}	3.9×10^{-3}	0.469	0.231	2.9	0.13
Min.	3.8×10^{-3}	1.2×10^{-3}	0.383	0.161	0.2	0.10
Max.	2.5×10^{-2}	8.8×10^{-3}	0.583	0.298	10.0	0.16
SD	8.9×10^{-3}	2.9×10^{-3}	0.065	0.054	3.6	0.02
		Layer 5 (n = 14)				
Mean	1.7×10^{-2}	9.4×10^{-3}	0.344	0.220	4.0	0.15
Min.	7.0×10^{-4}	4.0×10^{-4}	0.301	0.162	0.2	0.11
Max.	6.6×10^{-2}	3.6×10^{-2}	0.435	0.337	11.8	0.19
SD	1.8×10^{-2}	1.0×10^{-2}	0.044	0.051	3.8	0.02

Table 4. Descriptive statistics for fine-soil and field (soil plus rock fragments) saturated hydraulic conductivities (K_s and K_{sT}), fine-soil and field saturated water contents (θ_s and θ_{sT}), and Rossi-Nimmo retention model fitting parameters (ψ_o, λ) for layers within trench fill.

	K_s	K_{sT}	θ_s	θ_{sT}	ψ_o	λ
	cm/s		m^3/m^3		cm water	
		Layer 1 (n = 12)				
Mean	4.4×10^{-4}	2.8×10^{-4}	0.315	0.236	15.4	0.22
Min.	7.0×10^{-5}	5.8×10^{-5}	0.244	0.176	7.4	0.19
Max.	9.1×10^{-4}	5.5×10^{-4}	0.365	0.318	21.6	0.25
SD	2.6×10^{-4}	1.5×10^{-4}	0.037	0.047	3.9	0.02
		Layer 2 (n = 12)				
Mean	5.7×10^{-4}	3.6×10^{-4}	0.324	0.228	13.4	0.22
Min.	1.2×10^{-4}	7.6×10^{-5}	0.255	0.180	9.2	0.21
Max.	1.5×10^{-3}	9.0×10^{-4}	0.372	0.265	19.5	0.24
SD	4.0×10^{-4}	2.5×10^{-4}	0.028	0.022	3.6	0.01
		Layer 3 (n = 6)				
Mean	4.0×10^{-4}	2.4×10^{-4}	0.331	0.236	16.8	0.22
Min.	2.0×10^{-4}	1.4×10^{-4}	0.299	0.205	11.5	0.20
Max.	9.8×10^{-4}	5.4×10^{-4}	0.359	0.258	22.6	0.26
SD	2.9×10^{-4}	1.6×10^{-4}	0.022	0.021	4.3	0.02
		Layer 4 (n = 6)				
Mean	5.4×10^{-4}	3.0×10^{-4}	0.311	0.199	16.6	0.21
Min.	2.9×10^{-4}	1.3×10^{-4}	0.257	0.153	14.5	0.19
Max.	8.6×10^{-4}	5.3×10^{-4}	0.371	0.265	20.3	0.23
SD	2.2×10^{-4}	1.4×10^{-4}	0.048	0.038	2.7	0.02
		Layer 5 (n = 6)				
Mean	9.6×10^{-4}	6.2×10^{-4}	0.330	0.247	12.9	0.22
Min.	4.4×10^{-4}	2.9×10^{-4}	0.293	0.211	6.6	0.19
Max.	2.0×10^{-3}	1.2×10^{-3}	0.374	0.278	16.1	0.25
SD	7.0×10^{-4}	4.2×10^{-4}	0.028	0.024	4.2	0.02

Prior to applying ANOVA procedures, residual analyses were used to test ANOVA assumptions of normally distributed and homogeneous error and to determine the need for data transformation. Failure to meet one or more of the assumptions can affect significance levels and the sensitivity of the F test. Thus, without preliminary evaluation of residuals and, if needed, the application of appropriate remedial measures, ANOVA results could lead to incorrect conclusions. Except for clay content ($P < W = 0.007$) and K_{sT} ($P < W = 0.0001$), the physical and hydraulic properties had normally distributed error: $P < W$ values were 0.396 for silt, 0.593 for sand, 0.143 for R_v, 0.835 for ρ_T, 0.992 for θ_T, 0.967 for θ_{sT}, 0.272 for ψ_o, and 0.838 for λ. Residual plots (data not shown) also indicated variance heterogeneity for clay content and K_{sT}. Application of a log transformation to clay and K_{sT} data resulted in normal error distributions ($P < W = 0.562$ for log[clay]; $P < W = 0.781$ for log[K_{sT}]) and more homogeneous errors. The method of Box et al. (1978) confirmed that the log transformation was most appropriate for both properties.

The ANOVA results for physical properties are summarized in Table 5 and material × layer interaction means are shown in Fig. 2. The overall material × layer interaction effect was significant for each property except sand ($P > F = 0.072$). Orthogonal contrasts, which partition the overall interaction effect into four components, were used to provide more powerful tests of the specific layer-to-layer interactions that are of interest in this study. These contrasts show that at least one of the

Table 5. Summary of analysis of variance and orthogonal contrasts for testing effects of burial-trench construction on selected physical properties and vertical variability of these properties: log(clay), silt, sand, volumetric rock-fragment content (R_v), field (soil plus rock fragments) bulk density (ρ_T), and field water content (θ_T) during sampling.

Source of variation or contrast	df	Probability level ($P > F$) log(clay)	Silt	Sand	R_v	ρ_T	θ_T
Material (M)	1	0.033	0.048	0.105	0.043	0.244	0.020
Main-plot error	2	–	–	–	–	–	–
Layer (L)	4	0.0004	0.016	0.037	0.002	0.0001	0.001
M × L	4	0.004	0.048	0.072	0.023	0.0001	0.008
Orthogonal contrast†							
(M1L1 − M2L1) = (M1L2 − M2L2)	1	0.059	0.005	0.031	0.004	0.0001	0.392
(M1L2 − M2L2) = (M1L3 − M2L3)	1	0.002	0.263	0.035	0.692	0.0006	0.038
(M1L3 − M2L3) = (M1L4 − M2L4)	1	0.607	0.652	0.421	0.838	0.011	0.208
(M1L4 − M2L4) = (M1L5 − M2L5)	1	0.377	0.911	0.384	0.662	0.001	0.124
Split-plot error	8	–	–	–	–	–	–
Total	19	–	–	–	–	–	–

† Material × layer interaction means denoted by M_iL_j for the ith level of material (1 = soil; 2 = fill) and the jth level of layer (j = 1, 2, 3, 4, or 5).

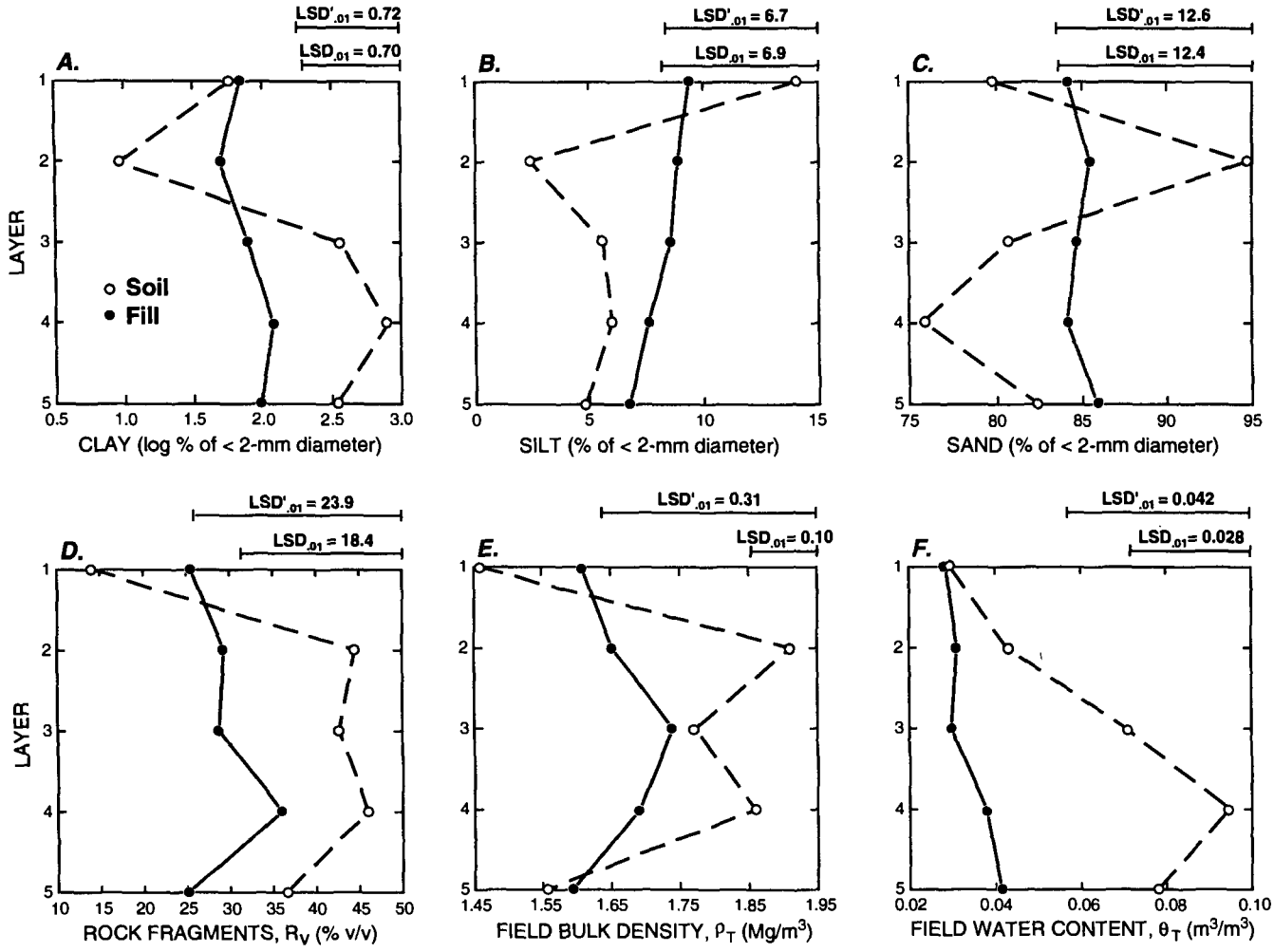

Fig. 2. Material × layer interaction means for selected physical properties: (A) log(clay), (B) silt, (C) sand, (D) volumetric rock-fragment content, (E) field (soil plus rock fragments) bulk density, and (F) field water content at time of sampling. Test statistics are: LSD(0.01) for comparing layer means within a material, and LSD'(0.01) for comparing material means within the same layer or different layers.

four individual material × contiguous layer interactions was significant for each of the physical properties considered under the ANOVA model (Table 5). For log(clay), silt, sand, R_v, and θ_T, the significant contrasts are attributed to large differences observed between contiguous soil Layers 1 and 2 or 2 and 3 (Fig. 2A, 2B, 2C, 2D, and 2F). Compared with the other physical properties, ρ_T, which is affected by both R_v and ρ_b, had the most significant layer-to-layer variability (four significant contrasts for ρ_T in Table 5; Fig. 2E).

Because of significant interactions, the material and layer effects on physical properties cannot be interpreted independently and differences between pairs of material × layer interaction mean values are evaluated using LSD and LSD'. For log(clay), silt, sand, R_v, and θ_T, no significant differences were observed among layers within trench fill (Fig. 2A, 2B, 2C, 2D, and 2F). The log(clay) value for soil Layer 2 was less than those for fill, whereas the value for soil Layer 4 was greater than those for fill (Fig 2A). For sand content, differences between soil and fill layers were not significant (Fig. 2C). Silt content and R_v values for soil Layer 1 were significantly different from values for the underlying soil layers, but differences between soil and fill layers typically were not significant (Fig 2B and 2D). Differences between θ_T values for the three deep soil layers and those for all other soil and fill layers typically were significant (Fig. 2F). Although the magnitude of variation in ρ_T values for the trench fill was less than for native soil, fill Layer 3 was significantly denser than Layers 1 and 5, and Layer 4 was denser than Layer 5.

The ANOVA results for hydraulic properties are summarized in Table 6 and material × layer interaction means are shown in Fig. 3. The overall material × layer interaction effect was not significant for $\log(K_{sT})$ and θ_{sT}, but was significant for ψ_o and λ. For each hydraulic property, however, contrasts indicated significant interaction between materials and contiguous Layers 1 and 2. The significance of these interactions is attributed to large differences between soil Layers 1 and 2 (Fig. 3). Within the native soil, differences between $\log(K_{sT})$ and θ_{sT} values for Layers 1 and 2 were significant and values for Layers 3, 4, and 5 were intermediate (Fig. 3A and 3B). In comparison with $\log(K_{sT})$ values for the soil, trench fill values were similar to soil Layer 1, but, in most cases, fill values were significantly less than those

Table 6. Summary of analysis of variance and orthogonal contrasts for testing effects of burial-trench construction on hydraulic properties and vertical variability of these properties: log(field [soil plus rock fragments] saturated hydraulic conductivity) (K_{sT}), field saturated water content (θ_{sT}), and Rossi-Nimmo retention model fitting parameter (ψ_o, λ).

Source of variation or contrast	df	Probability level ($P > F$)			
		$\log(K_{sT})$	θ_{sT}	ψ_o	λ
Material (M)	1	0.002	0.374	0.002	0.009
Main-plot error	2	–	–	–	–
Layer (L)	4	0.084	0.186	0.0004	0.002
M × L	4	0.178	0.201	0.0005	0.003
Orthogonal contrast†					
(M1L1 – M2L1) = (M1L2 – M2L2)	1	0.023	0.044	0.0002	0.0006
(M1L2 – M2L2) = (M1L3 – M2L3)	1	0.381	0.536	0.430	0.893
(M1L3 – M2L3) = (M1L4 – M2L4)	1	0.793	0.252	0.496	0.678
(M1L4 – M2L4) = (M1L5 – M2L5)	1	0.863	0.280	0.120	0.685
Split-plot error	8	–	–	–	–
Total	19	–	–	–	–

† Material × layer interaction means denoted by M_iL_j for the ith level of material (1 = soil; 2 = fill) and the jth level of layer (j = 1, 2, 3, 4, or 5).

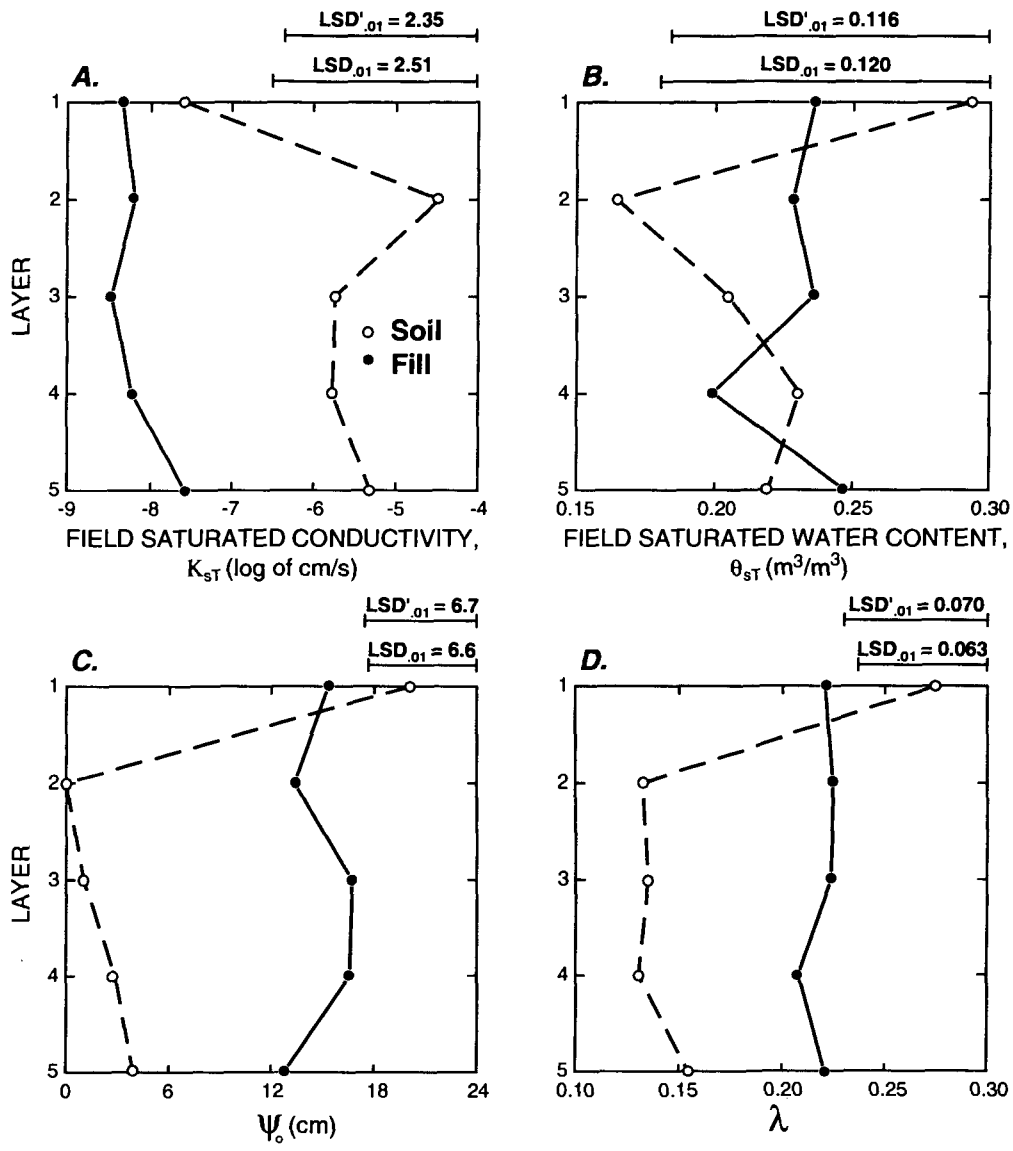

Fig. 3. Material × layer interaction means for hydraulic properties: (A) log(field [soil plus rock fragments] saturated hydraulic conductivity), (B) field saturated water content and fitting parameters for the Rossi-Nimmo retention model: (C) ψ_o is related to air-entry suction and (D) λ is a shape factor. Test statistics are: LSD(0.01) for comparing layer means within a material, and LSD'(0.01) for comparing material means within the same layer or different layers.

for the soil subsurface layers. Differences between soil and fill θ_{sT} values were not significant. For both water-retention fitting parameters, the soil Layer 1 value was significantly greater than those for the subsurface soil layers (Fig. 3C and 3D). Trench-fill values for ψ_o and λ typically were similar to those for soil Layer 1, but were significantly greater than those for soil subsurface layers.

Results of the statistical analyses clearly show that construction of waste-burial trenches had substantial effects on physical and hydraulic properties and their vertical variability. Steps used in the construction of burial trenches (excavation, stockpiling excavated materials, and backfilling) produced a fill material that was significantly less variable than the native soil. In addition, exposure of excavated soil to air produced a fill material that, on average, was drier than the undisturbed native soil (fill, 0.034 m^3 m^{-3}; soil, 0.063 m^3 m^{-3}). Surprisingly, such changes typically are not considered in the evaluation of proposed waste-burial sites. Most often, a great deal of effort is placed on characterizing flow and transport in the natural system with little regard as to whether the actual disposal facility will mimic the natural system. How changes to the natural system may affect flow processes at the Amargosa Desert site are discussed below under hydraulic properties of the conceptual model components.

Preliminary Conceptual Models of Vertical Variation within the Native Soil Profile and Trench Fill

The results of statistical analyses were used to quantitatively develop preliminary conceptual models of vertical variation within the native soil profile and trench fill. For the native soil profile, all the physical and hydraulic properties considered under the ANOVA model, except for θ_T measured during sampling, showed significant differences between Layers 1 and 2. Values for these two contiguous layers commonly represented the extremes for the soil profile. Differences between soil Layer 2 and the underlying layers were significant for several physical properties: log(clay), sand, ρ_T, and θ_T. Although means comparisons showed no differences between $\log(K_{sT})$ values for Layer 2 vs. Layer 3, 4, or 5, the trend was toward decreased conductivity for the three underlying layers ($P > |t| = 0.130$, 0.119, and 0.290, respectively). Similarly, comparisons between θ_{sT} values for Layer 2 vs. Layers 3, 4, and 5 showed a trend toward increased θ_{sT} for the three underlying layers ($P > |t| = 0.294$, 0.103, 0.163, respectively). Among the three deep soil layers, however, only ρ_T was found to differ significantly. Thus, on the basis of these statistical results, the preliminary conceptual model for the native soil profile is represented by three major components: Layer 1, Layer 2, and a composite of Layers 3, 4, and 5.

For the trench fill, except for ρ_T, none of the properties considered under the ANOVA model showed significant differences among layers. Therefore, the conceptual model of vertical variation within the trench fill is represented by a single composite of Layers 1, 2, 3, 4, and 5.

Hydraulic Properties of the Conceptual Model Components

Water-retention data and the Rossi–Nimmo retention model fitted with mean parameters for each component of the native soil profile and the trench fill conceptual models are shown in Fig. 4. Within the individual plots shown in Fig. 4, each symbol represents the mean of (A) 18, (B) 6, (C) 26, and (D) 42 subsample values determined using pressure-plate or water-activity meter methods. The 15 300-cm pressure-plate data, which were omitted from the hydraulic-property analysis, are shown to further demonstrate the apparent lack of equilibration for these measurements. For each of the conceptual model components, the water-activity meter measurements made immediately after the 15 300-cm pressure-plate measurements were significantly less than the expected 15 300-cm value ($P > |t| = 0.001$). Average differences were 8380 cm water for soil Layer 1, 5270 cm water for soil Layer 2, 9040 cm water for soil composite Layers 3, 4, and 5, and 8860 cm water for trench fill. Greater differences corresponded with finer textured material. Gee et al. (1992) suggested that the water-activity meter is best adapted for measurement of soils drier than 4080 cm water suction. Although water-activity measurements were not made immediately following the 5100-cm pressure-plate measurement, the data appear to be fairly continuous across this region. The results suggest that use of standard, 15 300-cm pressure-plate data for the lower limit of water-retention measurements may lead to significant errors in the description of hydraulic properties and prediction of water flow in dry soils.

Among the conceptual model components, soil Layer 2, the component with the coarsest texture, retained the least water. For suctions $<1 \times 10^3$ cm water, soil Layer 1 retained the greatest volume of water. For suctions $>1 \times 10^3$ cm water, however, the high clay content of soil composite Layers 3, 4, and 5 resulted in this component holding the greatest volume of water. The retention curve for trench fill was intermediate between soil Layer 1 and soil composite Layers 3, 4, and 5.

The ψ_j value determined for the Rossi–Nimmo model represents the second junction point where the fitted function deviates from the power law and becomes completely logarithmic. For each component of the conceptual models, the mean value for this analytically determined point [$\psi_j = \psi_d \exp(-1/\lambda)$] was: 2.4×10^5 cm water for soil Layer 1; 4.8×10^3 cm water for soil Layer 2; 8.2×10^3 cm water for soil composite Layers 3, 4, and 5; 9.8×10^4 cm water for trench fill.

As a check of the adequacy of the laboratory-derived water-retention functions, suction values for the Rossi–Nimmo model that correspond with θ_T values measured at the time of sampling were compared with suction values measured at the field site using psychrometers. For soil Layer 1 (initial $\theta_T = 0.030$ m^3 m^{-3}), the calculated suction value of 9.8×10^4 cm water (Fig. 4A) is consistent with field values that ranged from about 4.5×10^4 to $>8 \times 10^4$ cm water (upper limit of psychrometer calibration) (1987, unpublished data). For fill

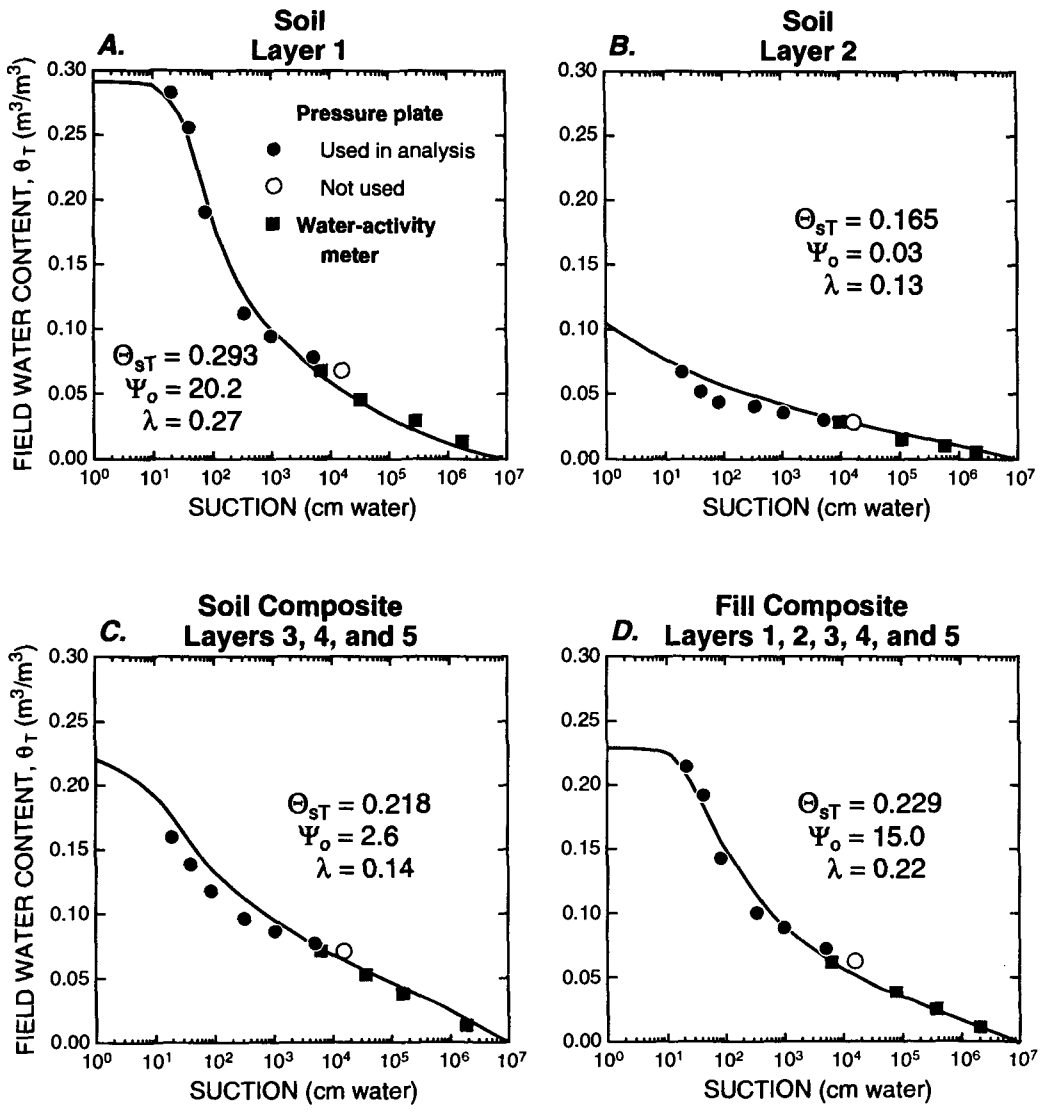

Fig. 4. Water-retention data and the Rossi-Nimmo model fitted with mean parameters and reported on a field (soil plus rock fragments) basis for each component of the conceptual models for native soil profile and trench fill. (A) soil, Layer 1; (B) soil, Layer 2; (C) soil, composite Layers 3, 4, and 5; and (D) fill, composite Layers 1, 2, 3, 4, and 5.

composite Layers 1, 2, 3, 4, and 5 (avg. initial θ_T = 0.034 m^3 m^{-3}), the calculated suction value of 8.7 × 10^4 cm water (Fig. 4D) also is consistent with field values of >8 × 10^4 cm (Andraski, 1990). For the two components that show more rapid release of water at low suctions (soil Layer 2, initial θ_T = 0.043 m^3 m^{-3}; soil composite Layers 3, 4, and 5, avg. initial θ_T = 0.081 m^3 m^{-3}), the agreement is not as good. Calculated suction values for these components are 9.3 × 10^2 and 3.1 × 10^3 cm water, respectively (Fig. 4B and 4C) compared with field values between 4 × 10^4 and 5 × 10^4 cm water (Fischer, 1992). Although this evaluation is limited to single points (initial values) on the respective retention curves, the agreement between laboratory-derived suction values and those measured in the field is reasonable, especially when considering that values are approaching the logarithmic part of the retention curve, where a small change in water content corresponds with a large change in suction.

Describing liquid hydraulic conductivity and vapor conductivity is important because of the low water contents measured at the site. Liquid hydraulic conductivity (K_l) of the fine soil may be described as a function of θ using the Rossi-Nimmo junction model (Eq. [2]) in combination with the capillary bundle model of Mualem (1976)

$$K_l(\theta) = K_s(\theta/\theta_s)^{1/2}\,[I(\theta)/I(\theta_s)]^2 \qquad [5]$$

where $I(\theta)$ is the integral for any value of θ between $\theta = 0$ and θ_s and $I(\theta_s)$ is the total integral from $\theta = 0$ to θ_s (Rossi and Nimmo, 1994). Mehuys et al. (1975) have shown that, if hydraulic conductivity is expressed as a function of ψ, unsaturated K_l values do not need to be corrected for rock-fragment content. Thus, the Mualem model was solved in terms of ψ by substituting Eq. [2] into Eq. [5] and expressing saturated hydraulic conductivity as K_{sT} (Eq. [1]). For this substitution, the integral for each of the three components of the retention

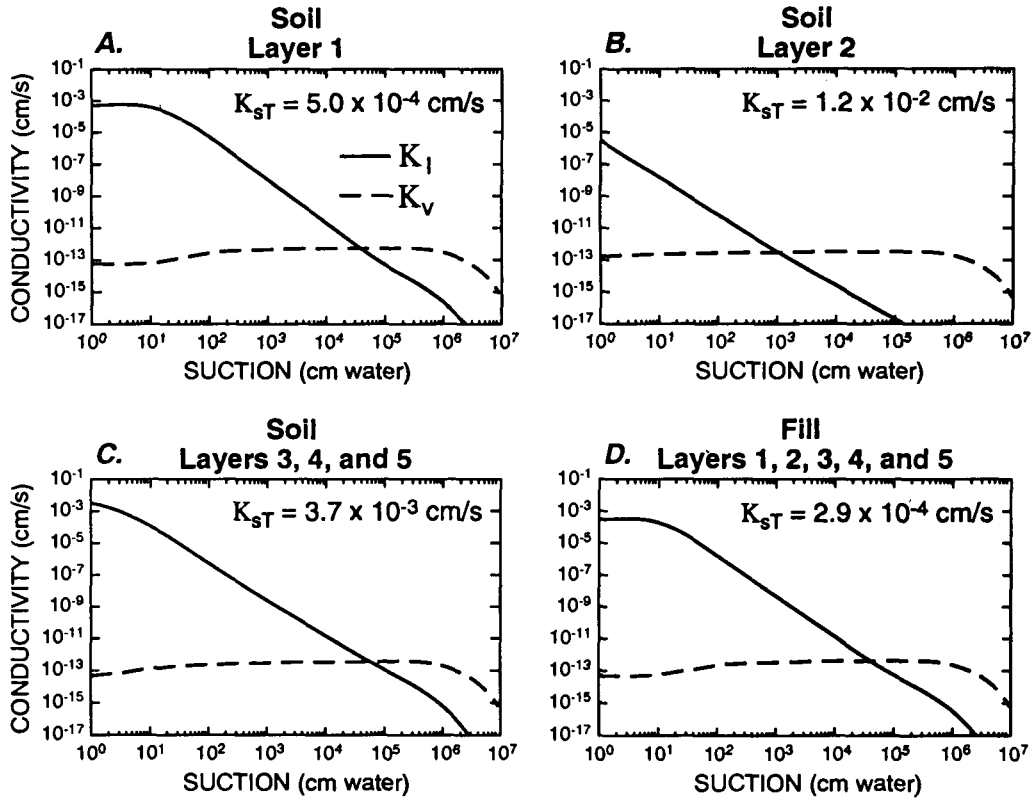

Fig. 5. Field (soil plus rock fragments) saturated hydraulic conductivity (K_{sT}), liquid hydraulic conductivity (K_l), and isothermal (20°C) vapor conductivity (K_v) as a function of suction for each component of the conceptual models for native soil profile and trench fill: (A) soil, Layer 1; (B) soil, Layer 2; (C) soil, composite Layers 3, 4, and 5; and (D) fill, composite Layers 1, 2, 3, 4, and 5.

model (I_{III}, I_{II}, and I_I) is expressed as

$$I_{III}(\psi) = (\alpha/\psi) - (\alpha/\psi_d) \quad \psi_d \geq \psi \geq \psi_j$$

$$I_{II}(\psi) = \{\lambda/[\psi_o(\lambda + 1)]\}\,[(\psi_o/\psi)^{\lambda+1} - (\psi_o/\psi_j)^{\lambda+1}] \quad \psi_j \geq \psi \geq \psi_i$$

$$I_I(\psi) = (2c/\psi_o^2)(\psi_i - \psi) \quad \psi_i \geq \psi \geq 0 \qquad [6]$$

Combining I_{III}, I_{II}, and I_I gives the integral $I(\psi)$ for any value of ψ,

$$I(\psi) = I_{III}(\psi) \quad \psi_d \geq \psi \geq \psi_j$$
$$I(\psi) = I_{III}(\psi_j) + I_{II}(\psi) \quad \psi_j \geq \psi \geq \psi_i$$
$$I(\psi) = I_{III}(\psi_j) + I_{II}(\psi_i) + I_I(\psi) \quad \psi_i \geq \psi \geq 0 \qquad [7]$$

and the total integral from $\psi = \psi_d$ to 0 cm water suction is

$$I(\psi_{total}) = I_{III}(\psi_j) + I_{II}(\psi_i) + I_I(0) \qquad [8]$$

Isothermal vapor conductivity (K_v) was described as a function of ψ using

$$K_v(\psi) = (D_v \rho_s Mg/\rho_w RT)\mathrm{RH} \qquad [9]$$

The derivation of Eq. [8] is described by Fayer et al. (1992). In Eq. [9], $K_v(\psi)$ is expressed in cm s^{-1}, D_v is diffusion coefficient for water vapor in soil (cm^2 s^{-1}), ρ_s is saturated water vapor density (g cm^{-3}), ρ_w is density of liquid water (g cm^{-3}), RH is relative humidity [RH = $\exp(-\psi Mg/RT)$], and M, g, R, and T are as defined in Eq. [3]. The diffusion coefficient accounts for tortuosity of the diffusion path and the reduced cross-sectional area for flow by $D_v = D_a \tau \varphi$, where D_a is diffusivity of water vapor in bulk air, τ is a tortuosity factor (assumed to be 0.66; Penman, 1940), and φ is air-filled porosity (total porosity minus θ_T). Calculations of K_v reported here are based on the assumption that θ_{sT} is 90% of total porosity.

The K_l and K_v functions for each component of the native soil profile and trench fill conceptual models are shown in Fig. 5. Accuracy of K_l calculated through Eq. [5] to [8] has not been tested. Comparison with the few data in the literature on hydraulic conductivity of dry soils, however, indicates the calculated values are quite reasonable. Mehuys et al. (1975) used a transient-outflow method to measure total hydraulic conductivity (K_l plus K_v) of three desert soils (a gravelly loamy sand and two gravelly sandy loam soils) within a suction range from 50 to 50 000 cm water. Their measured conductivity values ranged from about 10^{-4} to 10^{-11} cm s^{-1}. Conductivities calculated in this range of suction for soil Layer 1 (loamy sand), soil composite Layers 3, 4, and 5 (gravelly coarse sandy loam), and trench fill (gravelly loamy coarse sand) typically are within an order of magnitude of the values measured by Mehuys et al. (1975). For a sandy soil, Nimmo et al. (1992) used steady-state centrifuge methods to measure K_l values that ranged from about 10^{-6} cm s^{-1} at 100 cm water suction to 10^{-9} cm s^{-1} at 430 cm water suction. Recently, Mehta et al. (1994) measured total hydraulic conductivity of a dune sand from saturation to 2.5×10^5 cm water (θ = 0.01 m^3 m^{-3}) using a steady-state flux control and an instantaneous-profile method in two suction ranges. Across the

full suction range, their measured values ranged from about 10^{-2} to 10^{-13} cm s^{-1}. At suctions near 100 and 430 cm water, conductivity values measured by Mehta et al. (1994) ($\approx 10^{-9}$ and 10^{-10} cm s^{-1}, respectively) were less than those reported by Nimmo et al. (1992). At the lower and upper extremes of the suction range covered by Mehta et al. (1994), the sum of calculated K_l and K_v values for soil Layer 2, the coarse sand (Fig. 5B), duplicates their measured values within a factor of ≤ 2.3. At intermediate suctions, calculated values typically are about one to two orders of magnitude less than conductivities measured by Mehta et al. (1994) and three to four orders of magnitude less than those measured by Nimmo et al. (1992). Additional studies specifically designed to test the accuracy of predictive equations against direct measurements of unsaturated conductivity in dry soils are needed.

Among the conceptual model components for the Amargosa Desert site, K_{sT} was greatest for soil Layer 2, but with increased suction, values rapidly decreased to two to four orders of magnitude less than those for the other components (Fig. 5). The shape of the K_l functions for soil Layer 1 and the trench fill was similar, but across a suction range from 0 to about 1×10^4 cm water, K_l values for soil Layer 1 were about twice those for the trench fill.

The textural discontinuity between the two uppermost soil layers has been noted as important in impeding continued downward flow of water in the undisturbed native soil profile at the Amargosa Desert site (Gee et al., 1994). Although hydraulic conductivity typically is less for the trench fill than for the native surface soil, lack of textural discontinuity in the fill increases the potential for meteoric water to come in contact with and transport buried waste.

The K_v functions were similar for all model components, except at suctions <100 cm water, where K_v values were greater for soil Layer 2 (Fig. 5). The suction value at which K_v begins to exceed K_l differed among the conceptual model components: about 4×10^4 cm water for soil Layer 1 and the trench fill; 1×10^3 cm water for soil Layer 2; 6×10^4 cm water for soil composite Layers 3, 4, and 5. Thus, during trench construction, K_v was $\geq K_l$ for each of the model components except the deep (2–5 m) soil composite. Total hydraulic conductivity, however, was greater for the soil composite layer ($\approx 10^{-10}$ cm s^{-1}) than for the other model components ($\approx 10^{-13}$ cm s^{-1}).

Exposure of excavated soil to air during trench construction produced a fill material that was drier than the undisturbed native soil profile. Although this effect is considered transient, these dry initial conditions have strong implications concerning the relative importance of liquid flow vs. vapor flow processes in the body of burial trenches. Such initial conditions can be markedly altered, however, by the timing and quantity of precipitation and the subsequent redistribution and evaporation of infiltrated water. For example, results from field monitoring at the Amargosa Desert site (first 3 yr of a 5-yr study) showed that during the first year following trench construction, redistribution of infiltrated water caused suction values to decrease rapidly to about 1×10^3 cm water at depths of 0.6 to 0.75 m in native soil and to about 4.8×10^4 cm water at a depth of 0.75 m in the fill of the east trench (Gee et al., 1994). In the absence of vegetation, these decreased suction values persisted for the next 2 yr. Thus, depending on specific but commonly transient conditions, the relative importance of liquid flow and vapor flow as transport mechanisms for buried contaminants may differ dramatically.

Both liquid and vapor flow can occur as a consequence of matric suction and temperature gradients. Thermally induced liquid flow usually is not large enough to require consideration, but thermally induced vapor flow may be important where soils are dry and large temperature fluctuations occur (Campbell, 1985). Recently, Scanlon and Milly (1994) used numerical simulations to evaluate liquid- and vapor-flow processes in response to an annual climate cycle at an undisturbed site in the Chihuahuan Desert of Texas. Changes in water storage associated with individual rainfall events and subsequent evaporation were confined mainly to the top 0.3 m of soil. Total water flow in this soil zone was dominated by downward and upward liquid fluxes, which were driven by matric-suction gradients. Upward, isothermal-vapor flux dominated only in the top several millimeters of soil during periods of evaporation. Below the 0.3-m depth, simulated water fluxes varied relatively little. The dominant flow component, however, was thermal-vapor flux, which varied with season and depth in accordance with changes in the temperature gradient. The results of Scanlon and Milly (1994) demonstrate the complexity of flow processes that may occur in an undisturbed arid setting. Additional study is needed to evaluate how the natural flow system may be altered by the installation of a waste-burial facility.

SUMMARY AND CONCLUSIONS

Physical and hydraulic properties were determined for five layers within both the native soil profile (upper 5 m) and trench fill. Steps used in trench construction (excavation and stockpiling of native soil, backfilling with stockpiled soil) had a significant effect on soil properties and their variability. Surprisingly, such changes typically are not considered in the evaluation of proposed waste-burial sites. Most often, a great deal of effort is placed on characterizing flow and transport in the natural system with little regard as to whether the actual disposal facility will mimic the natural system. Results of statistical analyses were used to quantitatively develop preliminary conceptual models of vertical variation within the native soil profile and trench fill. The conceptual model for native soil is represented by three major horizontal components and the trench fill is represented by a single component.

Water retention measurements were extended to air dryness ($\psi = 2 \times 10^6$ cm water suction). Water-activity meter measurements made immediately after the 15 300-cm pressure-plate measurements showed the actual suction values were significantly less than the expected 15 300-cm value (avg. difference = 8550 ± 2460

cm water). This discrepancy is assumed to be due to lack of equilibration for the pressure-plate measurement and, therefore, the 15 300-cm pressure-plate data were omitted from hydraulic-property analysis. Water retention was modeled to oven dryness using the Rossi and Nimmo (1994) junction model. The junction model described the measured values well, and predicted suction values were consistent with field values. Calculated hydraulic conductivities also were in reasonable agreement with the few measured values of conductivity in dry soils that are reported in the literature.

Backfilling with the very dry material produced by the trench construction process, at least initially, will increase the importance of vapor flow as a transport mechanism in the trench fill. Although liquid hydraulic conductivity for the trench fill is about half that for the native surface soil at suctions $\leq 1 \times 10^4$ cm water, the lack of textural discontinuity in the fill may allow infiltrated water to continue downward, increasing the potential for meteoric water to come in contact with and transport buried waste.

Results of this study show that construction of waste-burial trenches can markedly alter the natural site environment. Such alterations must be considered in siting and designing arid waste-burial and monitoring systems and also in predicting the effectiveness of proposed sites and facilities for long-term waste isolation. This study quantitatively describes the hydraulic properties and vertical variations at a site using data measured across a water-content range that is representative of arid conditions, but is seldom studied. The data suggest that use of standard, 15 300-cm pressure-plate data for the lower limit of water-retention measurements may lead to significant errors in the description of hydraulic properties and prediction of water flow in dry soils. Results of the study provide data for physically based flow and solute-transport models intended to simulate processes in the near surface and at depth at a representative arid waste-burial site.

ACKNOWLEDGMENTS

The author acknowledges K.J. Hill and M.L. Tumbush for assistance in laboratory analysis; G.C.J. Fernandez, G.W. Gee, and S.W. Tyler for helpful discussions; and R.L. Sweet and J.V. Trionfante for editing and illustrations.

REFERENCES

Andraski, B.J. 1990. Water movement and trench stability at a simulated arid burial site for low-level radioactive waste near Beatty, Nevada. p. 166–173. *In* Proc. Conf. Nuclear waste isolation in the unsaturated zone, Las Vegas, NV. 17–21 Sept. 1989. Am. Nuclear Soc., LaGrange, IL.

Andraski, B.J. 1991. Balloon and core sampling for determining bulk density of alluvial desert soil. Soil Sci. Soc. Am. J. 55:1188–1190.

Andraski, B.J. 1992. Water movement through soil at a low-level radioactive waste site in the Amargosa Desert. p. 73–75. *In* U.S. Geol. Surv. Yearb. Fiscal Year 1991. U.S. Geol. Surv., Denver, CO.

Blake, G.R., and K.H. Hartge. 1986. Particle density. p. 377–382. *In* A. Klute (ed.) Methods of soil analysis. Part 1. 2nd ed. Agron. Monogr. 9. ASA and SSSA, Madison, WI.

Box, G.E.P, W.G. Hunter, and I.S. Hunter. 1978. Statistics for experimenters: An introduction to design, data analysis, and model building. John Wiley & Sons, New York.

Campbell, G.S. 1985. Soil physics with BASIC. Elsevier, New York.

Dunn, A.J., and G.R. Mehuys. 1984. Relationship between gravel content of soils and saturated hydraulic conductivity in laboratory tests. p. 55–63. *In* J.E. Box, Jr. (ed.) Erosion and productivity of soils containing rock fragments. SSSA Spec. Publ. 13. SSSA, Madison, WI.

Fayer, M.J., and G.W. Gee. 1992. Predicted drainage at a semiarid site: Sensitivity to hydraulic property description and vapor flow. p. 609–619. *In* M.Th. van Genuchten et al. (ed.) Indirect methods for estimating the hydraulic properties of unsaturated soils. Proc. Int. Workshop, Riverside, CA. 11–13 Oct. 1989. Univ. of California, Riverside.

Fayer, M.J., M.L. Rockhold, and M.D. Campbell. 1992. Hydrologic modeling of protective barriers: Comparison of field data and simulation results. Soil Sci. Soc. Am. J. 56:690–700.

Fernandez, G.C.J. 1992. Residual analysis and data transformations: Important tools in statistical analysis. Hortic. Sci. 27:297–300.

Fischer, J.M. 1992. Sediment properties and water movement through shallow unsaturated alluvium at an arid site for disposal of low-level radioactive waste near Beatty, Nye County, Nevada. Water Resour. Invest. Rep. 92-4032. U.S. Geol. Surv., Denver, CO.

Gee, G.W., and J.W. Bauder. 1986. Particle-size analysis. p. 383–411. *In* A. Klute (ed.) Methods of soil analysis. Part 1. 2nd ed. Agron. Monogr. 9. ASA and SSSA, Madison, WI.

Gee, G.W., M.D. Campbell, G.S. Campbell, and J.H. Campbell. 1992. Rapid measurement of low soil water potentials using a water activity meter. Soil Sci. Soc. Am. J. 56:1068–1070.

Gee, G.W., and D. Hillel. 1988. Groundwater recharge in arid regions: Review and critique of estimation methods. Hydrol. Process. 2:255–266.

Gee, G.W., P.J. Wierenga, B.J. Andraski, M.H. Young, M.J. Fayer, and M.L. Rockhold. 1994. Variations in water balance at three western desert sites. Soil Sci. Soc. Am. J. 58:63–72.

Istok, J.D., D.O. Blout, L. Barker, K.R. Johnejack, and D.P. Hammermeister. 1994. Spatial variability in alluvium properties at a low-level nuclear waste site. Soil Sci. Soc. Am. J. 58:1040–1051.

Klute, A. 1986. Water retention: Laboratory methods. p. 635–662. *In* A. Klute (ed.) Methods of soil analysis. Part 1. 2nd ed. Agron. Monogr. 9. ASA and SSSA, Madison, WI.

Klute, A., and C. Dirksen. 1986. Hydraulic conductivity and diffusivity: laboratory methods. p. 687–734. *In* A. Klute (ed.) Methods of soil analysis. Part 1. 2nd ed. Agron. Monogr. 9. ASA and SSSA, Madison, WI.

McFadden, L.D., S.G. Wells, and M.J. Jercinovich. 1987. Influences of eolian and pedogenic processes on the origin and evolution of desert pavements. Geology 15:504–508.

Mehta, B.K, S. Shiozawa, and M. Nakano. 1994. Hydraulic properties of a sandy soil at low water contents. Soil Sci. 157:208–214.

Mehuys, G.R, L.H. Stolzy, J. Letey, and L.V. Weeks. 1975. Effect of stones on the hydraulic conductivity of relatively dry desert soils. Soil Sci. Soc. Am. Proc. 39:37–42.

Mualem, Y. 1976. A new model for predicting the hydraulic conductivity of unsaturated porous media. Water Resour. Res. 12:513–522.

Nativ, R. 1991. Radioactive waste isolation in arid zones. J. Arid Environ. 20:129–140.

Nichols, W.D. 1987. Geohydrology of the unsaturated zone at the burial site for low-level radioactive waste near Beatty, Nye County, Nevada. Water-Supply Pap. 2312. U.S. Geol. Surv., Denver, CO.

Nimmo, J.R., K.C. Akstin, and K.A. Mello. 1992. Improved apparatus for measuring hydraulic conductivity at low water content. Soil Sci. Soc. Am. J. 56:1758–1761.

Penman, H.L. 1940. Gas and vapor movements in the soil: I. The diffusion of vapors through porous solids. J. Agric. Sci. (Cambridge) 30:437–462.

Reith, C.C., and B.M. Thomson. 1992. Deserts as dumps? The disposal of hazardous materials in arid ecosystems. Univ. of New Mexico Press, Albuquerque.

Ross, P.J., J. Williams, and K.L. Bristow. 1991. Equation for extending water-retention curves to dryness. Soil Sci. Soc. Am. J. 55:923–927.

Rossi, C., and J.R. Nimmo. 1994. Modeling of soil water retention from saturation to oven dryness. Water Resour. Res. 30:701–708.

Russo, D. 1983. Leaching characteristics of a stony desert soil. Soil Sci. Soc. Am. J. 47:431-438.

SAS Institute. 1988. SAS/STAT user's guide. Version 6.04 ed. SAS Inst., Cary, NC.

Scanlon, B.R., and P.C.D. Milly. 1994. Water and heat fluxes in desert soils. 2. Numerical simulations. Water Resour. Res. 30: 721-733.

Steel, R.G., and J.H. Torrie. 1980. Principles and procedures of statistics. McGraw-Hill, New York.

Wood, J.L., and B.J. Andraski. 1995. Selected meteorological data for an arid site near Beatty, Nye County, Nevada, calendar years 1990 and 1991. Open-File Rep. 94-489. U.S. Geol. Surv., Denver, CO.

Published January, 1996

ERRATUM

Properties and Variability of Soil and Trench Fill at an Arid Waste-Burial Site

B.J. ANDRASKI

Soil Sci. Soc. Am. J. 60:54–66 (January-February 1996).

On p. 55, after Eq. [3], unit conversion for gas constant should have read erg = 10^{-7} J.